www.czasopisma.pan.pl PAN POLSKA AKADEMIA NAUK www.journals.pan.pl

Arch. Metall. Mater. **67** (2022), 1, 121-126

DOI: https://doi.org/10.24425/amm.2022.137480

M. BERENDT-MARCHEL[1], D. SIEMIASZKO[1*]

THE INFLUENCE OF IRON AND ALUMINIUM POWDER PRESSING ON THE COURSE OF SHRINKAGE AND PROPERTIES OF THE Fe40Al PHASE OBTAINED BY REACTION SINTERING

The effect of the compaction rate on the structure, microstructure and properties of Fe-Al sinters obtained during the SHS reaction is presented in this paper. It was found that increasing the uniaxial pressing pressure led to the increase of the contact area between iron and aluminium particles, which improved the conduction and lowered heat losses during the self-propagating high-temperature synthesis (SHS) reaction and thus result with a sintered material with an improved phase homogeneity. On the other hand, an increase in the pressing pressure causes air be trapped in the pores and later on reacts with iron and aluminium to form oxides. In this work, the shrinkage course was analysed at six different pressing pressures: 50, 100, 150, 200, 300 and 400 MPa. The green compacts were then subjected to the PAIS process (pressure-assisted induction sintering) at a temperature of 1000°C under a load of 100 kN for 5 min. Such prepared samples were subjected to density, porosity, and microhardness (HV0.1) measurements. X-ray diffraction phase analysis and SEM observations were performed together with EDS chemical composition measurements. For studied chemical composition of the samples and sample geometry, 200 MPa compacting pressure was found to be optimal in order to obtain the best sample homogeneity.

Keywords: intermetallic; powder metallurgy; reaction sintering; mechanical properties

1. Introduction

Intermetallic alloys from the iron-aluminium system have been known since the end of the nineteenth century. The basic method of manufacturing these materials is melting and casting. This process is carried out in arc or induction furnaces with the use of a protective atmosphere in the form of an inert gas or a vacuum. Melting and casting in air is limited due to the strong affinity of aluminium to oxygen, which leads to the formation of unfavourable aluminium oxides [1-5]. Additionally, due to the presence of water vapor in the air, hydrogen is released, which remains in the alloy, causing considerable hydrogen embrittlement [6,7]. The use of modern Exo-Melt casting techniques [8] allows improved control of the chemical composition of the alloy and also improves the safety of the smelting process.

The second main technique for the production of alloys from the Fe-Al system is powder metallurgy. The alloy powder or elementary powders of iron and aluminium can be used as the starting material. However, the use of an alloy powder is associated with substantial difficulties. The powder is expensive because the FeAl phase must first be formed and then crushed. In addition, the sintering process itself must be run at a high temperature, which leads to high energy costs. The formation of the FeAl phase directly from iron and aluminium powders is much more promising. Both powders are widely available and inexpensive [9]. Moreover, aluminium is a plastic material that allows the easy creation of a green compact. FeAl phase formation takes place at a much lower temperature, 660°C, which is the melting temperature of aluminium. The issue that complicates the whole process is the violent reaction between iron and aluminium [5,10]. This is a classic SHS (self-propagating high-temperature synthesis) reaction. Since the specific volume of the FeAl phase is smaller than the sum of the original powder volumes, porosity occurs in the sintered material. This results in a decrease in the strength and hardness of the material. The only way to eliminate porosity is to apply an additional load.

The sintering of phases from the Fe-Al system under loading is widely known in the literature [11-15]. However, there are no comprehensive studies describing the effect of compaction on the structure and properties of the obtained sinters in which the SHS reaction takes place. This is a very interesting and important issue. The selection of an optimal pressing pressure is influenced by a number of factors. Raising the pressing pressure increases the contact area between the iron and aluminium particles, which

[1] MILITARY UNIVERSITY OF TECHNOLOGY, 2 GEN. SYLWESTRA KALISKIEGO STR., 00-908 WARSZAWA, POLAND

* Correspondin author: dariusz.siemiaszko@wat.edu.pl

should lead to decreased heat losses during the SHS reaction and thus a sintered material with an improved phase homogeneity. To obtain a material with a density close to the theoretical density, many authors propose the use of a load up to 8 GPa [16,17]. On the other hand, an increase in the pressing pressure causes the air to become enclosed in the pores, which then, having no outlet, reacts with iron and aluminium to form oxides. The presence of oxides in the structure causes deterioration of the fracture toughness. In addition, as is known in the industry, the use of a high pressing pressures causes technical problems related to, for example, scratched dies. It leads to the rapid wear of the dies as well as the need to use presses that apply a significant pressure. In practice, when producing metallic structural elements, the pressure is usually not higher than 500 MPa.

The purpose of this work was to analyse the shrinkage course as a function of the pressing pressure and determine the lowest possible pressing pressure that produces a uniform structure in the material and also maintains properties in it that are as high as possible.

2. Materials and methods

A mixture of iron and aluminium powders in the ratio of Fe:Al 60:40 was used to create the Fe40Al phase and carry out the tests. The powders were mixed in a turbulent mixer for 30 min. The exact characteristics of the powders are given in [18]. The finished mixture was divided into 6 equal parts and pressed using the following pressures: 50, 100, 150, 200, 300 and 400 MPa. The green compacts were then subjected to the PAIS process (pressure-assisted sintering induction) at a temperature of 1000°C under a load of 100 kN for 5 min. The PAIS sintering took place in a vacuum chamber, while the die with the compact was additionally subjected to one-sided press loading. During sintering, the temperature and shrinkage changes at a frequency of 2 Hz were recorded simultaneously. A detailed description of the method of temperature measurement is given in [19].

The prepared samples were used to measure the density and porosity using the Archimedes method and microhardness measurements (HV0.1) using the Vickers method. The microstructure of the sintered compacts was observed and an analysis of the chemical compositions in micro-areas was also conducted using a Quanta FEG scanning electron microscope with an EDS detector.

XRD tests were carried out on a Rigaku-Ultima IV diffractometer using Co Kα1 as the radiation source. Measurements were made in the range from 20°-130° at a scan speed of 1 deg/min with a step of 0.02°. Subsequently, the resulting diffractograms were indexed on the basis of identification cards contained in the PDF-4 + 2014 database.

3. Results and discussion

Fig. 1a shows the course of the sintering process of the pressed compacts under pressures of 50, 100, 150, 200, 300 and 400 MPa. By analysing the diagrams below, it can be seen that in each case, the course of shrinkage is divided into three distinct stages. The first stage takes place before the SHS reaction is seen here as a temperature jump during heating. This stage is characterized by a high rate of shrinkage. Shrinkage in the second stage, after the SHS reaction, is small and amounts to approximately 5%. The last stage is the thermal shrinkage occurring after the start of cooling. It grows gradually as the temperature of the sintered compact. Upon analysing the presented graphs, it can be observed that the main changes that occur in the shrinkage take place before the SHS reaction (Fig. 1b). These changes involve both the shrinkage size and the initiation temperature. Generally, the lower the pressing pressure is, the greater the shrinkage, which is an obvious effect resulting from the removal of part of the porosity during the compaction stage of the compact. However, as shown in Fig. 2, shrinkage after the reaction (stage II + III marked with a dark green colour) is practically unchanged regardless of the pressure. The shrinkage value in this stage is constant and amounts to approx. 8-10%. Only the shrinkage in Stage I changes from 25% to approx. 7%, as marked in the light green colour.

Another effect apparent in Fig. 1b is that a reduction in the compact pressure leads to the beginning of the shrinkage starting earlier, i.e., at a lower temperature. Fig. 3a shows a method of reading the temperature at the beginning and end of the first stage of shrinkage. The start temperature was the temperature at which

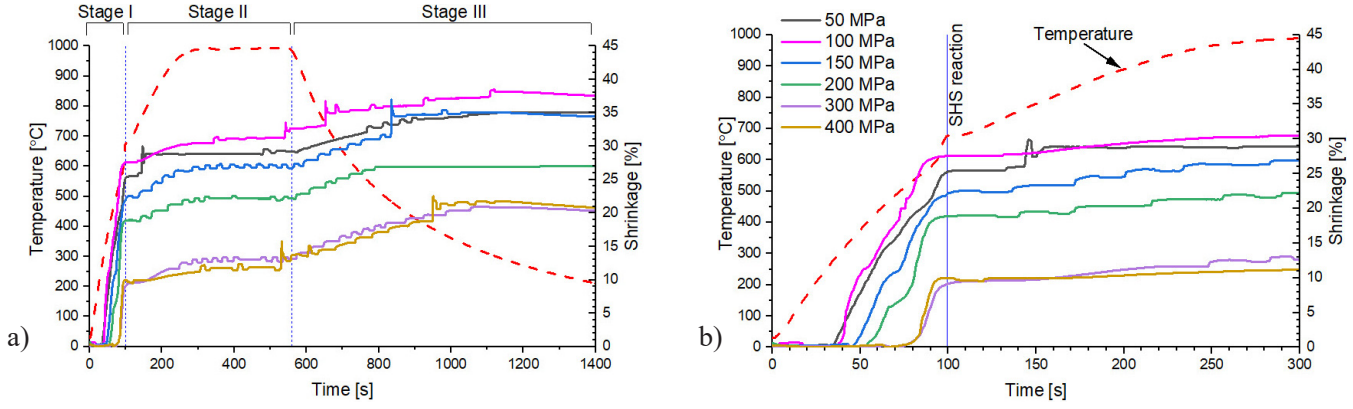

Fig. 1. The course of the sintering process (temperature and shrinkage) of pressed compacts under the pressure: a) the whole process, b) first stage

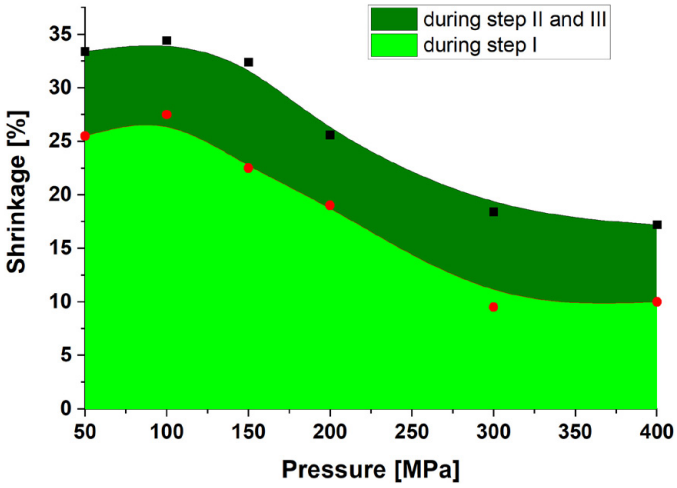

Fig. 2. The value of shrinkage before (light green) and after the reaction (dark green)

the shrinkage began. The end temperature occurred when the SHS reaction completed. From an analysis of the changes in the temperature at the beginning and end of the first stage of shrinkage (Fig. 3b), it can be concluded that the temperature at the end of the shrinkage process remains constant. The value of this temperature is approximately 680°C, which corresponds to the temperature immediately after the SHS reaction. On the other hand, the temperature the beginning of shrinkage increases from 260°C to 500°C with an elevated pressing pressure of 300 MPa. A further increase in pressure does not increase in the temperature of the beginning of the shrinkage process. The low value of the starting temperature of shrinkage at small pressures is caused by the porosity present in the sinters. When the compact pressed under low pressure is subjected to heating, aluminium begins to plasticize and fill the pores present in the structure, which is visible as shrinkage. In the case of compacts pressed with high pressures, the large pores are already reduced during the compacting stage. Only small pores remain in the volume. For aluminium to fill them, it must be plastic, and hence, it should be heated to an elevated temperature.

The dependence of the relative density as a function of the pressure is shown in Fig. 4. Nearly all sintered compacts have a high-density value above 94%. At the same time, there is a certain upward trend with increasing pressing pressure. The density value increases from 94.8% (50 MPa) to 97.1% (300 MPa). The main pores present in the tested sinters are closed (dark green). With an increase in the pressing pressure, the porosity value drops from 5% at a pressure of 50 MPa to less than 4% at

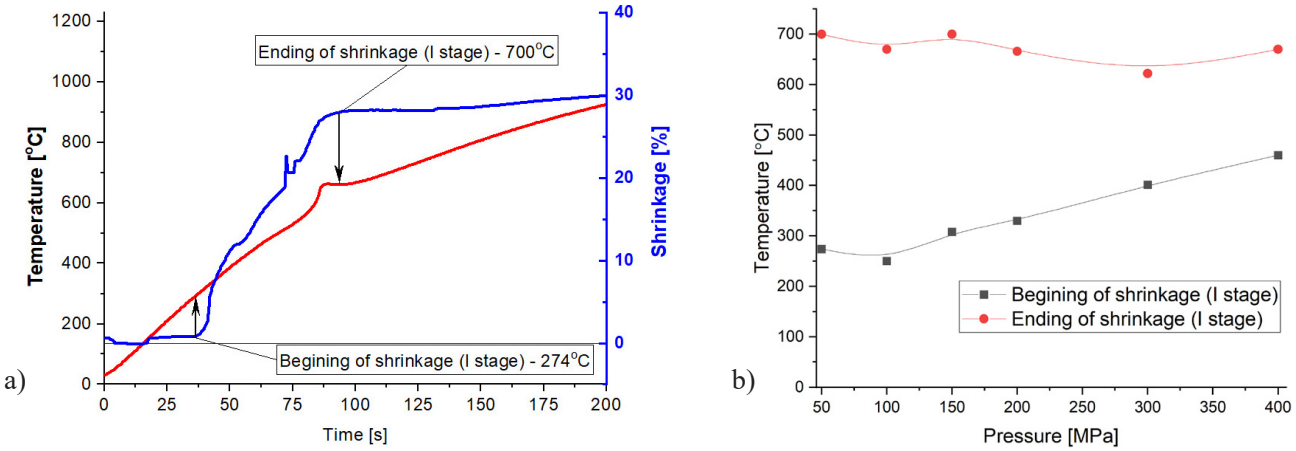

Fig. 3. A diagram for method of reading the temperature of the beginning and end of the first stage of shrinkage (a) and changes of the temperature of the beginning and end of the first stage of shrinkage (b)

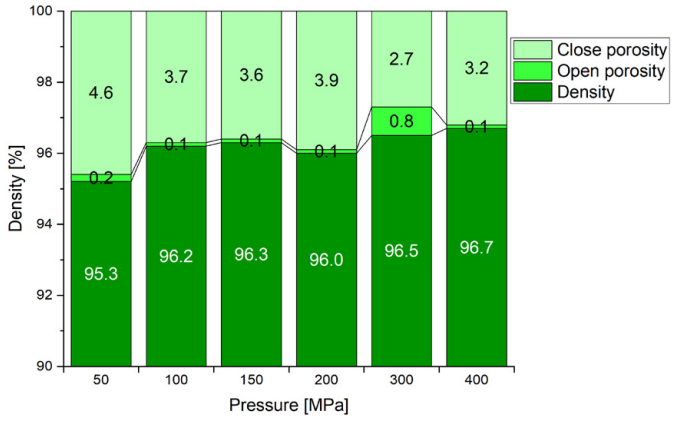

Fig. 4. The dependence of the relative density and porosity on the value of the compaction pressure

a pressure of 400 MPa. However, the open pores in the sinters (light green) are small and amount to a maximum of 0.8%. The observed decrease in the amount of closed pores confirms earlier conclusions regarding the closing of large pores in the structures of the sintered materials.

The diffractograms of the obtained materials are shown in Fig. 5. Two phases are identified in the sintered materials: FeAl and $FeAl_2$. The predominant phase is FeAl; however, the presence of low-intensity peaks from the $FeAl_2$ phase means that further heating is necessary for complete homogenization. This is confirmed by the microstructure observations (Fig. 6). Increasing the homogenization of the microstructure with increasing pressing pressure is visible. However, the images suggest a much greater heterogeneity than the results from the XRD analysis.

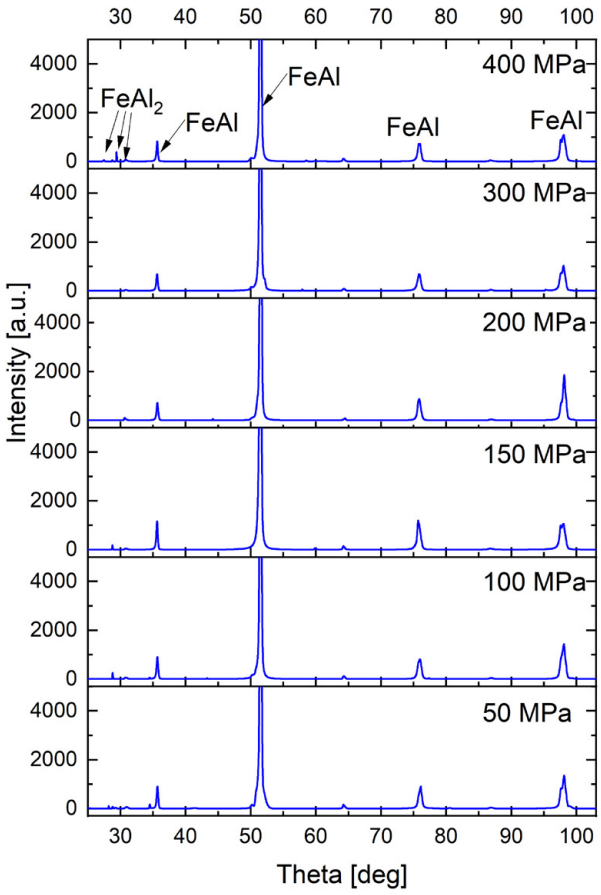

Fig. 5. The XRD patterns of the obtained materials

This is because the FeAl phase occurs over a wide range of aluminium contents, i.e. from about 36% to 51%. The change in the content of aluminium in the sintered materials is visible as a change in the colour in the SEM images in BSE mode.

This is confirmed by the EDS results. In the low-pressure compacted sample (50 MPa, Fig. 7a) areas with a chemical composition corresponding to several phases were identified: FeAl, several areas including the $FeAl_2$ phase and areas with an aluminium solution in iron – Fe(Al). For the high-pressure compacted sample (300 MPa, Fig. 7b) no phase with a high aluminium content ($FeAl_2$) was found. Only the target FeAl phase and areas with an aluminium solution in iron occurred.

The microhardness measurements are shown in Fig. 8. Each point indicates an individual result. Because each of the Fe-Al phases is characterized by different hardness values, the distributions of the results indicate the homogeneity of the sample. Based on the literature data [20-23], a dark green area corresponding to the microhardness of the high-aluminium phases is marked. Similarly, the area comprising FeAl is marked with a light green colour. The average value of the microhardness decreases significantly from 426 HV0.1 for 50 MPa to less than 300 HV0.1 for 400 MPa (the average hardness is marked on the graph by a black line). However, the reduction in the microhardness is not linear. There is a rapid increase in the microhardness between densities of 150 and 200 MPa. The microhardness of samples compressed with pressures less than 200 MPa is approximately 400 HV0.1, while samples compressed at 200 MPa decrease to

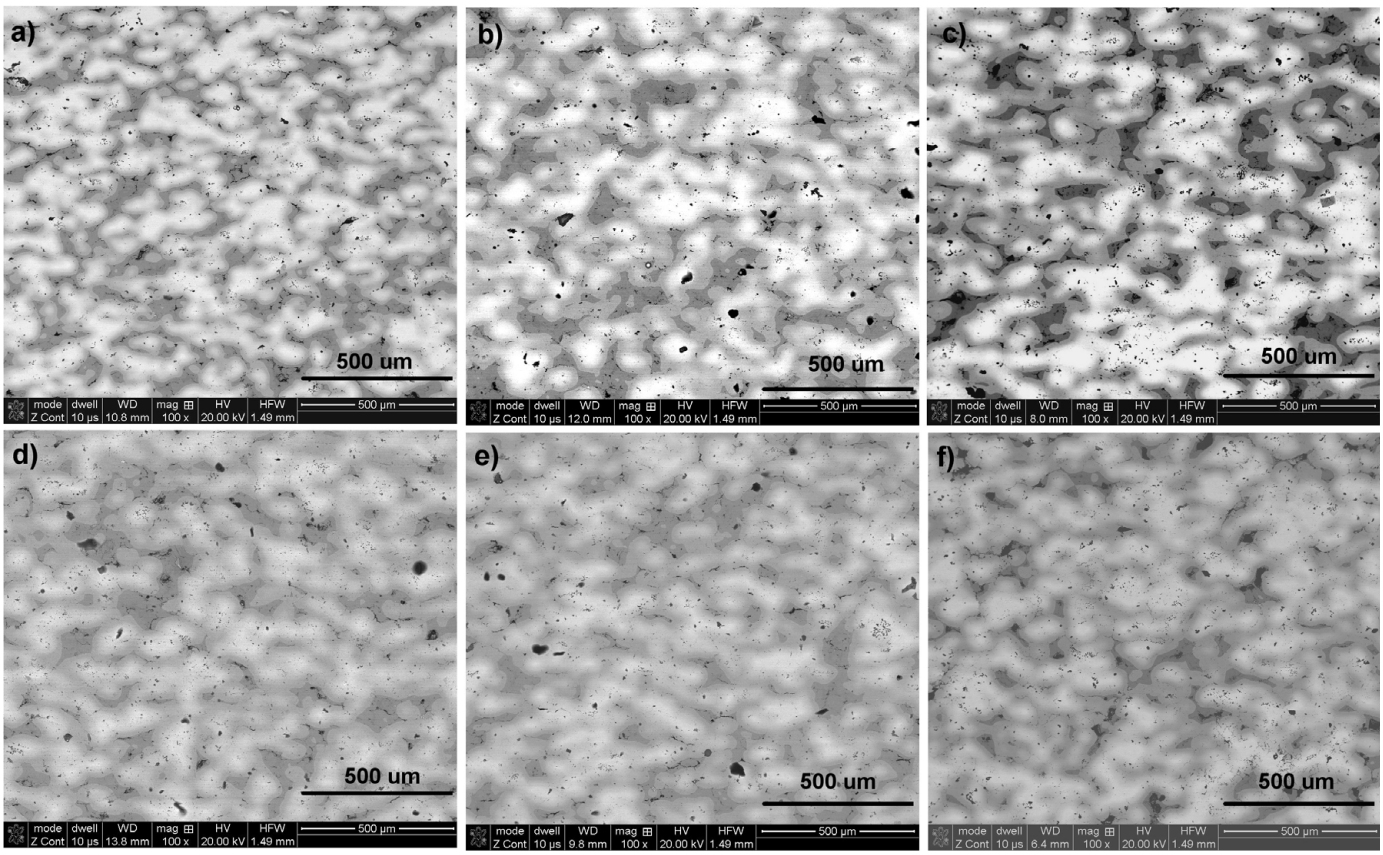

Fig. 6. The effect of compaction pressure on the microstructure of the sintered materials. The microstructure after compaction: 50 MPa (a), 100 MPa (b), 150 MPa (c), 200 MPa (d), 300 MPa (e) and 400 MPa (f)

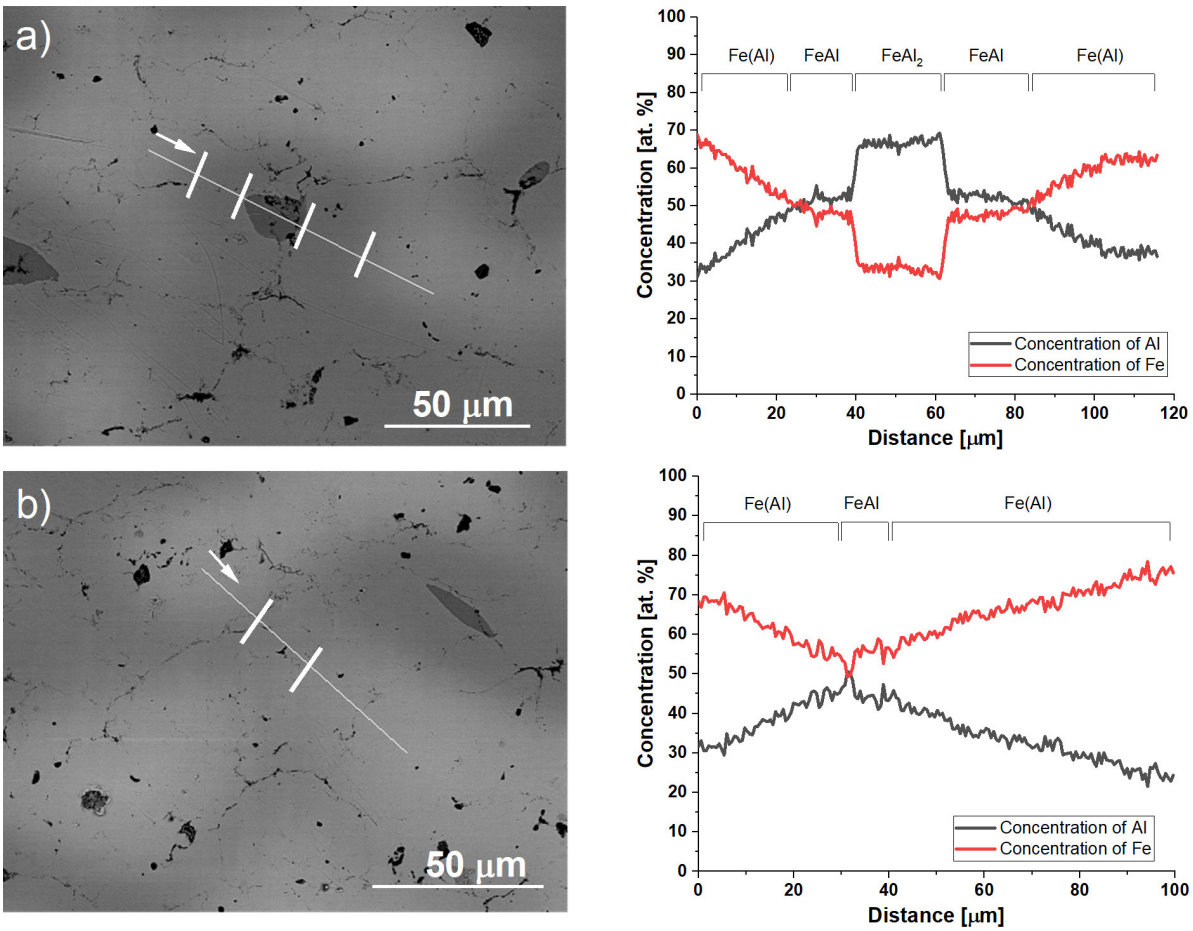

Fig. 7. Changes in chemical composition of the samples compacts under the pressure 50 MPa (a) and 300 MPa (b)

approximately 300 HV0.1. This means that when compacting at 200 MPa or more, the structure is much more homogeneous. This confirms the hardness values corresponding to high-aluminium phases at sintered pressures of 50 and 100 MPa. In the sample sintered at 150 MPa, there are transient results, and above 150 MPa the hardness values are less than 600 HV0.1. The homogenization of the structure may be the result of a reduced number of pores in the structure of the iron sintered at high pressures. Direct contact of iron with aluminium enables the formation of FeAl phases, which confirms the results obtained by X-ray phase analysis.

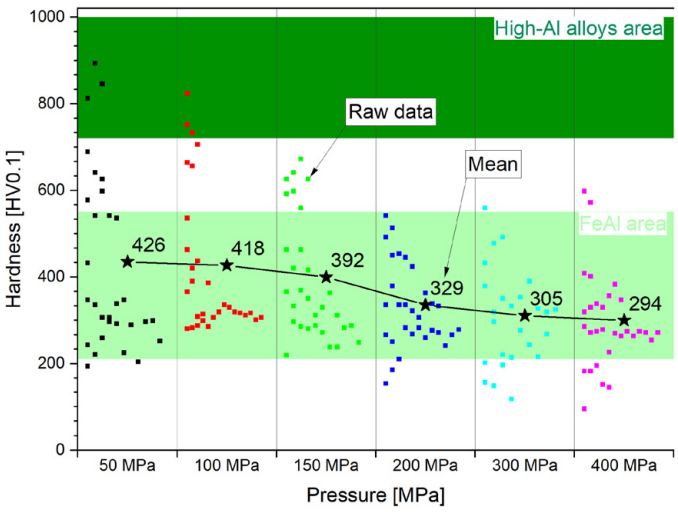

Fig. 8. The effect of the compaction pressure on average microhardness and its scatter

4. Summary

The presented results show that the compaction pressure of the compacts significantly influences the structure and properties of Fe40Al sinters obtained by the PAIS method. The shrinkage value before the SHS reaction decreases and the temperature of the onset of shrinkage increase with as the pressing pressure increases. This indicates the disappearance of large pores in the sintered structure. This results in a decrease in the porosity and hence an increase in the sintered density at increasing pressing pressures. The decrease in the porosity in the sintered compacts increases their homogenization and improves their mechanical properties. Microhardness, XRD, and EDS analyses showed that the proportion of high-aluminium phases in the structure decreases as the pressing pressure increases. The conducted research showed that the compaction pressure of 50-100 MPa is too low. This specimen has a heterogeneous structure and demonstrates the worst parameters herein. The optimal compact pressure for the green compacts is a pressure of approx. 200 MPa.

Acknowledgements

The project was funded by the National Science Center, Poland granted by decision number 2016/23/B/ST8/02126

REFERENCES

[1] C.T. Liu, J. Stringer, J.N. Mundy, L.L. Horton, P. Angelini, Intermetallics **5** (8), 579-596 (1997). DOI: https://doi.org/10.1016/S0966-9795(97)00045-9

[2] S.C. Deevi, V.K. Sikka, Intermetallics **4** (5), 357-375 (1996). DOI: https://doi.org/10.1016/0966-9795(95)00056-9

[3] C.T. Liu, E.P. George, P.J. Maziasz, J.H. Schneibel, Mater. Sci. Eng. **258** (1), 84-98 (1998). DOI: https://doi.org/10.1016/S0921-5093(98)00921-6

[4] S. Jóźwiak, K. Karczewski, Z. Bojar, Intermetallics **33**, 99-104 (2013). DOI: https://doi.org/10.1016/j.intermet.2012.10.003

[5] H.J. Grabke, Intermetallics **7** (10), 1153-1158 (1999). DOI: https://doi.org/10.1016/S0966-9795(99)00037-0

[6] V.K. Sikka, D. Wilkening, J. Liebetrau, B. Mackey, Mater. Sci. Eng. A, **258** (1), 229-235 (1998). DOI: https://doi.org/10.1016/S0921-5093(98)00938-1

[7] R.S. Sundar, R.G. Baligidad, Y.V.R.K. Prasad, D.H. Sastry, Mater. Sci. Eng. A, **258** (1), 219-228 (1998). DOI: https://doi.org/10.1016/S0921-5093(98)00937-X

[8] S.C. Deevi, V.K. Sikka, Intermetallics **5** (1), 17-27 (1997). DOI: https://doi.org/10.1016/S0966-9795(96)00067-2

[9] V.K. Sikka, S. Deevi, J.D. Vought, Mater. Sci. Forum. **147** (6), 29-31 (1995).

[10] T. Sritharan, S. Murali, P. Hing, Mater. Lett. **51** (6), 455-460 (2001). DOI: https://doi.org/10.1016/S0167-577X(01)00335-4

[11] S. Jóźwiak, K. Karczewski, Z. Bojar, Int. J. Powder. Metall. **45** (4), 40-44 (2009).

[12] S. Maki, Y. Harada, K. Mori, J. Mater. Process. Tech. **119** (1), 210-215 (2001). DOI: https://doi.org/10.1016/S0924-0136(01)00962-1

[13] S. Grasso, Y. Sakka, G. Maizza, Sci. Technol. Adv. Mat. **10** (5), 053001 (2009). DOI: https://doi.org/10.1088/1468-6996/10/5/053001

[14] T. Skiba, P. Haušild, M. Karlík, K. Vanmeensel, J. Vleugels, Intermetallics **18** (7), 1410-1414 (2010). DOI: https://doi.org/10.1016/j.intermet.2010.02.009

[15] D. Siemiaszko, J. Kuzia, Intermetallics **104**, 16-23 (2019). DOI: https://doi.org/10.1016/j.intermet.2018.10.009

[16] E. Godlewska, S. Szczepanik, R. Mania, J. Krawiarz, S. Koziński, Intermetallics **11** (4), 307-312 (2003). DOI: https://doi.org/10.1016/s0966-9795(02)00247-9

[17] E. Menéndez, J. Sort, M. Liedke, J. Fassbender, S. Suriñach, M. Baró, J. Nogues, New. J. Phys. **10**, 103030 (2008). DOI: https://doi.org/10.1088/1367-2630/10/10/103030

[18] D. Siemiaszko, B. Kowalska, P. Jozwik, M. Kwiatkowska, Materials **8** (4), 1513-1525 (2015). DOI: https://doi.org/2015/03/3110.3390/ma8041513

[19] D. Siemiaszko, R. Mościcki, J. Alloy. Compd. **632** (Supplement C), 335-342 (2015). DOI: https://doi.org/10.1016/j.jallcom.2014.11.163

[20] M.J. Torkamany, S. Tahamtan, J. Sabbaghzadeh, Mater. Design. **31** (1), 458-465 (2010). DOI: https://doi.org/10.1016/j.matdes.2009.05.046

[21] R. Wang, Y. Zhao, Z. Li, H. Chen, X. Tao, Y. Ouyang, Mater. Res. Express **5** (2), 026512 (2018). DOI: https://doi.org/10.1088/2053-1591/aaabda

[22] H. Ozaki, M. Kutsu, Welding Processes, INTECH, Rijeka (2012).

[23] I. Shishkovsky, F. Missemer, N. Kakovkina, I. Smurov, Crystals **3** (4), 517-529 (2013). DOI: https://doi.org/10.3390/cryst3040517